

VARIATIONAL IMBALANCED REGRESSION

Ziyan Wang

School of Industrial and Systems Engineering
Georgia Institute of Technology
Atlanta, GA 30332, USA
wzy@gatech.edu

Hao Wang

Department of Computer Science
Rutgers University
Piscataway, NJ 08854, USA
hogue.wang@rutgers.edu

ABSTRACT

Existing regression models tend to fall short in both accuracy and uncertainty estimation when the label distribution is imbalanced. In this paper, we propose a probabilistic deep learning model, dubbed variational imbalanced regression (VIR), which not only performs well in imbalanced regression but naturally produces reasonable uncertainty estimation as a byproduct. Different from typical variational autoencoders assuming I.I.D. representations (a data point’s representation is not directly affected by other data points), our VIR borrows data with similar regression labels to compute the latent representation’s variational distribution; furthermore, different from deterministic regression models producing point estimates, VIR predicts the entire normal-inverse-gamma distributions and modulates the associated conjugate distributions to impose probabilistic reweighting on the imbalanced data, thereby providing better uncertainty estimation. Experiments in several real-world datasets show that our VIR can outperform state-of-the-art imbalanced regression models in terms of both accuracy and uncertainty estimation.

1 INTRODUCTION

Deep regression models are currently the state of the art in making predictions in a continuous label space and have a wide range of successful applications in computer vision (Yin et al., 2021), natural language processing (Jiang et al., 2020), etc. However, these models fail however when the label distribution in training data is imbalanced. For example, in visual age estimation (Moschoglou et al., 2017), where a model infers the age of a person given her visual appearance, models are typically trained on imbalanced datasets with overwhelmingly more images of younger adults, leading to poor regression accuracy for images of children or elderly people (Yang et al., 2021). Such unreliability in imbalanced regression settings motivates the need for both *improving performance for the minority* in the presence of imbalanced data and, more importantly, *providing reasonable uncertainty estimation* to inform practitioners on how reliable the predictions are (especially for the minority where accuracy is lower).

Existing methods for deep imbalanced regression (DIR) only focus on improving the accuracy of deep regression models by smoothing the label distribution and reweighting data with different labels (Yang et al., 2021). On the other hand, methods that provide uncertainty estimation for deep regression models operates under the balance-data assumption and therefore do not work well in the imbalanced setting (Amini et al., 2020; Mi et al., 2022b; Charpentier et al., 2022).

To simultaneously cover these two desiderata, we propose a probabilistic deep imbalanced regression model, dubbed variational imbalanced regression (VIR). Different from typical variational autoencoders assuming I.I.D. representations (a data point’s representation is not directly affected by other data points), our VIR assumes Neighboring and Identically Distributed (N.I.D.) and borrows data with similar regression labels to compute the latent representation’s variational distribution. Specifically, VIR first encodes a data point into a probabilistic representation and then mix it with neighboring representations (i.e., representations from data with similar regression labels) to produce its final probabilistic representation; VIR is therefore particularly useful for minority data as it can borrow probabilistic representations from data with similar labels (and naturally weigh them using our probabilistic model) to counteract data sparsity. Furthermore, different from deterministic regression models producing point estimates, VIR predicts the entire normal-inverse-gamma distributions

and modulates the associated conjugate distributions by the importance weight computed from the smoothed label distribution to impose probabilistic reweighting on the imbalanced data. This allows the negative log likelihood to naturally put more focus on the minority data, thereby balancing the accuracy for data with different regression labels. Our VIR framework is compatible with any deep regression models and can be trained end to end.

We summarize our contributions as below:

- We identify the problem of probabilistic deep imbalanced regression as well as two desiderata, balanced accuracy and uncertainty estimation, for the problem.
- We propose VIR to simultaneously cover these two desiderata and achieve state-of-the-art performance compared to existing methods.
- As a byproduct, we also provide strong baselines for benchmarking high-quality uncertainty estimation and promising prediction performance on imbalanced datasets.

2 RELATED WORK

Variational Autoencoder. Variational autoencoder (VAE) (Kingma & Welling, 2014) is an unsupervised learning model that aims to infer probabilistic representations from data. However, as shown in Figure 1, VAE typically assumes I.I.D. representations, where a data point’s representation is not directly affected by other data points. In contrast, our VIR borrows data with similar regression labels to compute the latent representation’s variational distribution.

Imbalanced Regression. Imbalanced regression is under-explored in the machine learning community. Most existing methods for imbalanced regression are direct extensions of the SMOTE algorithm (Chawla et al., 2002), a commonly used algorithm for imbalanced classification, where data from the minority classes is over-sampled. These algorithms usually synthesize augmented data for the minority regression labels by either interpolating both inputs and labels (Torgo et al., 2013) or adding Gaussian noise (Branco et al., 2017; 2018) (more discussion on augmentation-based methods in the Supplementary).

Such algorithms fail to measure the distance in continuous label space and fall short in handling high-dimensional data (e.g., images and text). Recently, DIR (Yang et al., 2021) addresses these issues by applying kernel density estimation to smooth and reweight data on the continuous label distribution, achieving state-of-the-art performance. However, DIR only focuses on improving the accuracy, especially for the data with minority labels, and therefore does not provide uncertainty estimation, which is crucial to assess the predictions’ reliability. Ren et al. (2022) focuses on re-balancing the mean squared error (MSE) loss for imbalanced regression, and Gong et al. (2022) introduces ranking similarity for improving deep imbalanced regression. In contrast, our VIR provides a principled probabilistic approach to simultaneously achieve these two desiderata, not only improving upon DIR in terms of performance but also producing reasonable uncertainty estimation as a much-needed byproduct to assess model reliability. There is also related work on imbalanced classification (Deng et al., 2021), which is related to our work but focusing on classification rather than regression.

Uncertainty Estimation in Regression. There has been renewed interest in uncertainty estimation in the context of deep regression models (Kendall & Gal, 2017; Kuleshov et al., 2018; Song et al., 2019; Zelikman et al., 2020; Amini et al., 2020; Mi et al., 2022b; van Amersfoort et al., 2021; Liu et al., 2020; Gal & Ghahramani, 2016; Stadler et al., 2021; Snoek et al., 2019; Heiss et al.,

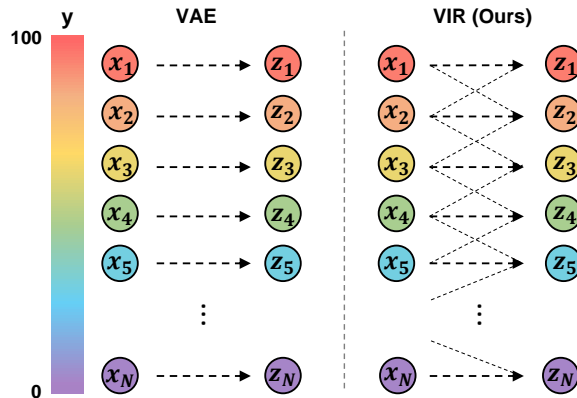


Figure 1: Comparison on inference networks between typical VAE (Kingma & Welling, 2014) and our VIR. In VAE (**left**), a data point’s latent representation (i.e., z) is affected only by itself, while in VIR (**right**), neighbors participate to modulate the final representation.

2021). Most existing methods either directly predict the variance of the output distribution as the estimated uncertainty (Kendall & Gal, 2017; Zhang et al., 2019; Amini et al., 2020) or rely on post-hoc confidence interval calibration (Kuleshov et al., 2018; Song et al., 2019; Zelikman et al., 2020). Closest to our work is Deep Evidential Regression (DER) (Amini et al., 2020), which attempts to estimate both aleatoric and epistemic uncertainty (Kendall & Gal, 2017; Hüllermeier & Waegeman, 2019) on regression tasks by training the neural networks to directly infer the parameters of the evidential distribution, thereby producing uncertainty measures. DER (Amini et al., 2020) is designed for the data-rich regime and therefore fails to reasonably estimate the uncertainty if the data is imbalanced; for data with minority labels, DER (Amini et al., 2020) tends produce unstable distribution parameters, leading to poor uncertainty estimation (as shown in Sec. 5). In contrast, our proposed VIR explicitly handles data imbalance in the continuous label space to avoid such instability; VIR does so by modulating both the representations and the output conjugate distribution parameters according to the imbalanced label distribution, allowing training/inference to proceed as if the data is balance and leading to better performance as well as uncertainty estimation (as shown in Sec. 5).

3 METHOD

In this section we introduce the notation and problem setting, provide an overview of our VIR, and then describe details on each of VIR’s key components.

3.1 NOTATION AND PROBLEM SETTING

Assuming an imbalanced dataset in continuous space $\{\mathbf{x}_i, y_i\}_{i=1}^N$ where N is the total number of data points, $\mathbf{x}_i \in \mathbb{R}^d$ is the input, and $y_i \in \mathcal{Y} \subset \mathbb{R}$ is the corresponding label from a continuous label space \mathcal{Y} . In practice, \mathcal{Y} is partitioned into B equal-interval bins $[y^{(0)}, y^{(1)}), [y^{(1)}, y^{(2)}), \dots, [y^{(B-1)}, y^{(B)}]$, with slight notation overload. To directly compare with baselines, we use the same grouping index for target value $b \in \mathcal{B}$ as in (Yang et al., 2021). We denote representations as \mathbf{z}_i , and use $(\tilde{\mathbf{z}}_i^\mu, \tilde{\mathbf{z}}_i^\Sigma) = q_\phi(\mathbf{z}|\mathbf{x}_i)$ to denote the probabilistic representations for input \mathbf{x}_i generated by a probabilistic encoder parameterized by ϕ ; furthermore, we denote $\bar{\mathbf{z}}$ as the mean of representation \mathbf{z}_i in each bin, i.e., $\bar{\mathbf{z}} = \frac{1}{N_b} \sum_{i=1}^{N_b} \mathbf{z}_i$ for a bin with N_b data points. Similarly we use (\hat{y}_i, \hat{s}_i) to denote the mean and variance of the predictive distribution generated by a probabilistic predictor $p_\theta(y_i|\mathbf{z})$.

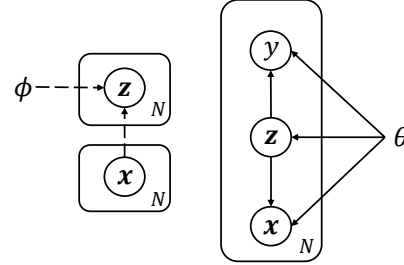


Figure 2: Overview of our VIR method. **Left:** The inference model infers the latent representations given input \mathbf{x} ’s in the neighborhood. **Right:** The generative model reconstructs the input and predicts the label distribution (including the associated uncertainty) given the latent representation.

3.2 METHOD OVERVIEW

In order to achieve both desiderata in probabilistic deep imbalanced regression (i.e., performance improvement and uncertainty estimation), our proposed variational imbalanced regression (VIR) operates on both the encoder $q_\phi(\mathbf{z}_i|\{\mathbf{x}_i\}_{i=1}^N)$ and the predictor $p_\theta(y_i|\mathbf{z}_i)$.

Typical VAE (Kingma & Welling, 2014) lower-bounds input \mathbf{x}_i ’s marginal likelihood; in contrast, VIR lower-bounds the marginal likelihood of input \mathbf{x}_i and labels y_i :

$$\log p_\theta(\mathbf{x}_i, y_i) = \mathcal{D}_{\mathcal{KL}}(q_\phi(\mathbf{z}_i|\{\mathbf{x}_i\}_{i=1}^N)||p_\theta(\mathbf{z}_i|\mathbf{x}_i, y_i)) + \mathcal{L}(\theta, \phi; \mathbf{x}_i, y_i).$$

Note that our variational distribution $q_\phi(\mathbf{z}_i|\{\mathbf{x}_i\}_{i=1}^N)$ (1) does not condition on labels y_i , since the task is to predict y_i and (2) conditions on all (neighboring) inputs $\{\mathbf{x}_i\}_{i=1}^N$ rather than just \mathbf{x}_i . The second term $\mathcal{L}(\theta, \phi; \mathbf{x}_i, y_i)$ is VIR’s evidence lower bound (ELBO), which is defined as:

$$\mathcal{L}(\theta, \phi; \mathbf{x}_i, y_i) = \underbrace{\mathbb{E}_q[\log p_\theta(\mathbf{x}_i|\mathbf{z}_i)]}_{\mathcal{L}_i^{\mathcal{P}}} + \underbrace{\mathbb{E}_q[\log p_\theta(y_i|\mathbf{z}_i)]}_{\mathcal{L}_i^{\mathcal{P}}} - \underbrace{\mathcal{D}_{\mathcal{KL}}(q_\phi(\mathbf{z}_i|\{\mathbf{x}_i\}_{i=1}^N)||p_\theta(\mathbf{z}_i))}_{\mathcal{L}_i^{\mathcal{KL}}}. \quad (1)$$

where the $p_\theta(\mathbf{z}_i)$ is the standard Gaussian prior $\mathcal{N}(\mathbf{0}, \mathbf{I})$, following typical VAE (Kingma & Welling, 2014), and the expectation is taken over $q_\phi(\mathbf{z}_i|\{\mathbf{x}_i\}_{i=1}^N)$, which infers \mathbf{z}_i by borrowing data with similar regression labels to produce the balanced probabilistic representations, which is beneficial especially for the minority (see Sec. 3.3 for details).

Different from typical regression models which produce only point estimates for y_i , our VIR’s predictor, $p_\theta(y_i|\mathbf{z}_i)$, directly produces the parameters of the entire NIG distribution for y_i and further imposes probabilistic reweighting on the imbalanced data, thereby producing balanced predictive distributions (more details in Sec. 3.4).

3.3 CONSTRUCTING $q(\mathbf{z}_i|\{\mathbf{x}_i\}_{i=1}^N)$

To cover both desiderata, one needs to (1) produce *balanced* representations to improve performance for the data with minority labels and (2) produce *probabilistic* representations to naturally obtain reasonable uncertainty estimation for each model prediction. To learn such *balanced probabilistic representations*, we construct the encoder of our VIR (i.e., $q_\phi(\mathbf{z}_i|\{\mathbf{x}_i\}_{i=1}^N)$) by (1) first encoding a data point into a **probabilistic representation**, (2) computing **probabilistic statistics** from neighboring representations (i.e., representations from data with similar regression labels), and (3) producing the final representations via **probabilistic whitening and recoloring** using the obtained statistics.

Intuition on Using Probabilistic Representation. DIR uses deterministic representations, with one vector as the final representation for each data point. In contrast, our VIR uses probabilistic representations, with one vector as the mean of the representation and another vector as the variance of the representation. Such dual representation is more robust to noise and therefore leads to better prediction performance. Therefore, We first encode each data point into a probabilistic representation. Note that this is in contrast to existing work (Yang et al., 2021) that uses deterministic representations. We assume that each encoding \mathbf{z}_i is a Gaussian distribution with parameters $\{\mathbf{z}_i^\mu, \mathbf{z}_i^\Sigma\}$, which are generated from the last layer in the deep neural network.

From I.I.D. to Neighboring and Identically Distributed (N.I.D.). Typical VAE (Kingma & Welling, 2014) is an unsupervised learning model that aims to learn a variational representation from latent space to reconstruct the original inputs under the I.I.D. assumption; that is, in VAE, the latent value (i.e., \mathbf{z}_i) is generated from its own input \mathbf{x}_i . This I.I.D. assumption works well for data with majority labels, but significantly harms performance for data with minority labels. To address this problem, we replace the I.I.D. assumption with the N.I.D. assumption; specifically, VIR’s variational latent representations still follow Gaussian distributions (i.e., $\mathcal{N}(\mathbf{z}_i^\mu, \mathbf{z}_i^\Sigma)$), but these distributions will be first calibrated using data with neighboring labels. For a data point (\mathbf{x}_i, y_i) where y_i is in the b ’th bin, i.e., $y_i \in [y^{(b-1)}, y^{(b)})$, we compute $q(\mathbf{z}_i|\{\mathbf{x}_i\}_{i=1}^N) \triangleq \mathcal{N}(\mathbf{z}_i; \tilde{\mathbf{z}}_i^\mu, \tilde{\mathbf{z}}_i^\Sigma)$ with the following four steps.

- (1) Mean and Covariance of Initial \mathbf{z}_i : $\mathbf{z}_i^\mu, \mathbf{z}_i^\Sigma = \mathcal{I}(\mathbf{x}_i)$,
- (2) Statistics of Bin b ’s Statistics: $\boldsymbol{\mu}_b^\mu, \boldsymbol{\mu}_b^\Sigma, \boldsymbol{\Sigma}_b^\mu, \boldsymbol{\Sigma}_b^\Sigma = \mathcal{A}(\{\mathbf{z}_i^\mu, \mathbf{z}_i^\Sigma\}_{i=1}^N)$,
- (3) Smoothed Statistics of Bin b ’s Statistics: $\tilde{\boldsymbol{\mu}}_b^\mu, \tilde{\boldsymbol{\mu}}_b^\Sigma, \tilde{\boldsymbol{\Sigma}}_b^\mu, \tilde{\boldsymbol{\Sigma}}_b^\Sigma = \mathcal{S}(\{\boldsymbol{\mu}_b^\mu, \boldsymbol{\mu}_b^\Sigma, \boldsymbol{\Sigma}_b^\mu, \boldsymbol{\Sigma}_b^\Sigma\}_{b=1}^B)$,
- (4) Mean and Covariance of Final \mathbf{z}_i : $\tilde{\mathbf{z}}_i^\mu, \tilde{\mathbf{z}}_i^\Sigma = \mathcal{F}(\mathbf{z}_i^\mu, \mathbf{z}_i^\Sigma, \boldsymbol{\mu}_b^\mu, \boldsymbol{\mu}_b^\Sigma, \boldsymbol{\Sigma}_b^\mu, \boldsymbol{\Sigma}_b^\Sigma, \tilde{\boldsymbol{\mu}}_b^\mu, \tilde{\boldsymbol{\mu}}_b^\Sigma, \tilde{\boldsymbol{\Sigma}}_b^\mu, \tilde{\boldsymbol{\Sigma}}_b^\Sigma)$,

where the details of functions $\mathcal{I}(\cdot)$, $\mathcal{A}(\cdot)$, $\mathcal{S}(\cdot)$, and $\mathcal{F}(\cdot)$ are described below.

(1) Function $\mathcal{I}(\cdot)$: From Deterministic to Probabilistic Statistics. Different from deterministic statistics in (Yang et al., 2021), our VIR’s encoder uses *probabilistic statistics*, i.e., *statistics of statistics*. Specifically, VIR treats \mathbf{z}_i as a distribution with the mean and covariance $(\mathbf{z}_i^\mu, \mathbf{z}_i^\Sigma) = \mathcal{I}(\mathbf{x}_i)$ rather than a deterministic vector.

As a result, all the deterministic statistics for bin b , $\boldsymbol{\mu}_b$, $\boldsymbol{\Sigma}_b$, $\tilde{\boldsymbol{\mu}}_b$, and $\tilde{\boldsymbol{\Sigma}}_b$ are replaced by distributions with the means and covariances, $(\boldsymbol{\mu}_b^\mu, \boldsymbol{\mu}_b^\Sigma)$, $(\boldsymbol{\Sigma}_b^\mu, \boldsymbol{\Sigma}_b^\Sigma)$, $(\tilde{\boldsymbol{\mu}}_b^\mu, \tilde{\boldsymbol{\mu}}_b^\Sigma)$, and $(\tilde{\boldsymbol{\Sigma}}_b^\mu, \tilde{\boldsymbol{\Sigma}}_b^\Sigma)$, respectively (more details in the following three paragraphs on $\mathcal{A}(\cdot)$, $\mathcal{S}(\cdot)$, and $\mathcal{F}(\cdot)$).

(2) Function $\mathcal{A}(\cdot)$: Statistics of the Current Bin b ’s Statistics. In VIR, the *deterministic overall mean* for bin b (with N_b data points), $\boldsymbol{\mu}_b = \bar{\mathbf{z}} = \frac{1}{N_b} \sum_{i=1}^{N_b} \mathbf{z}_i$, becomes the *probabilistic overall mean*, i.e., a distribution of $\boldsymbol{\mu}_b$ with the mean $\boldsymbol{\mu}_b^\mu$ and covariance $\boldsymbol{\mu}_b^\Sigma$ (assuming diagonal covariance) as

follows:

$$\begin{aligned}\boldsymbol{\mu}_b^\mu &\triangleq \mathbb{E}[\bar{\mathbf{z}}] = \frac{1}{N_b} \sum_{i=1}^{N_b} \mathbb{E}[\mathbf{z}_i] = \frac{1}{N_b} \sum_{i=1}^{N_b} \mathbf{z}_i^\mu, \\ \boldsymbol{\mu}_b^\Sigma &\triangleq \mathbb{V}[\bar{\mathbf{z}}] = \frac{1}{N_b^2} \sum_{i=1}^{N_b} \mathbb{V}[\mathbf{z}_i] = \frac{1}{N_b^2} \sum_{i=1}^{N_b} \mathbf{z}_i^\Sigma.\end{aligned}$$

Similarly, the *deterministic overall covariance* for bin b , $\boldsymbol{\Sigma}_b = \frac{1}{N_b} \sum_{i=1}^{N_b} (\mathbf{z}_i - \bar{\mathbf{z}})^2$, becomes the *probabilistic overall covariance*, i.e., a matrix-variate distribution (Gupta & Nagar, 2018) with the mean:

$$\boldsymbol{\Sigma}_b^\mu \triangleq \mathbb{E}[\boldsymbol{\Sigma}_b] = \frac{1}{N_b} \sum_{i=1}^{N_b} \mathbb{E}[(\mathbf{z}_i - \bar{\mathbf{z}})^2] = \frac{1}{N_b} \sum_{i=1}^{N_b} \left[\mathbf{z}_i^\Sigma + (\mathbf{z}_i^\mu)^2 - \left([\boldsymbol{\mu}_b^\Sigma]_i + ([\boldsymbol{\mu}_b^\mu]_i)^2 \right) \right],$$

since $\mathbb{E}[\bar{\mathbf{z}}] = \boldsymbol{\mu}_b^\mu$ and $\mathbb{V}[\bar{\mathbf{z}}] = \boldsymbol{\mu}_b^\Sigma$. Note that the covariance of $\boldsymbol{\Sigma}_b$, i.e., $\boldsymbol{\Sigma}_b^\Sigma \triangleq \mathbb{V}[\boldsymbol{\Sigma}_b]$, involves computing the fourth-order moments, which is computationally prohibitive. Therefore in practice, we directly set $\boldsymbol{\Sigma}_b^\Sigma$ to zero for simplicity; empirically we observe that such simplified treatment already achieves promising performance improvement upon the state of the art.

(3) Function $\mathcal{S}(\cdot)$: Neighboring Data and Smoothed Statistics. Next, we can borrow data from neighboring label bins b' to compute the smoothed statistics of the current bin b by applying a symmetric kernel $k(\cdot, \cdot)$ (e.g., Gaussian, Laplacian, and Triangular kernels). Specifically, the *probabilistic smoothed mean and covariance* are (assuming diagonal covariance):

$$\tilde{\boldsymbol{\mu}}_b^\mu = \sum_{b' \in \mathcal{B}} k(y_b, y_{b'}) \boldsymbol{\mu}_{b'}^\mu, \quad \tilde{\boldsymbol{\mu}}_b^\Sigma = \sum_{b' \in \mathcal{B}} k^2(y_b, y_{b'}) \boldsymbol{\mu}_{b'}^\Sigma, \quad \tilde{\boldsymbol{\Sigma}}_b^\mu = \sum_{b' \in \mathcal{B}} k(y_b, y_{b'}) \boldsymbol{\Sigma}_{b'}^\mu.$$

(4) Function $\mathcal{F}(\cdot)$: Probabilistic Whitening and Recoloring. We develop a probabilistic version of the whitening and re-coloring procedure in (Yang et al., 2021; Sun et al., 2016). Specifically, we produce the final probabilistic representation $\{\tilde{\mathbf{z}}_i^\mu, \tilde{\mathbf{z}}_i^\Sigma\}$ for each data point as:

$$\tilde{\mathbf{z}}_i^\mu = (\mathbf{z}_i^\mu - \boldsymbol{\mu}_b^\mu) \cdot \sqrt{\frac{\tilde{\boldsymbol{\Sigma}}_b^\mu}{\boldsymbol{\Sigma}_b^\mu}} + \tilde{\boldsymbol{\mu}}_b^\mu, \quad \tilde{\mathbf{z}}_i^\Sigma = (\mathbf{z}_i^\Sigma + \boldsymbol{\mu}_b^\Sigma) \cdot \sqrt{\frac{\tilde{\boldsymbol{\Sigma}}_b^\Sigma}{\boldsymbol{\Sigma}_b^\Sigma}} + \tilde{\boldsymbol{\mu}}_b^\Sigma. \quad (2)$$

During training, we keep updating the probabilistic overall statistics, $\{\boldsymbol{\mu}_b^\mu, \boldsymbol{\mu}_b^\Sigma, \boldsymbol{\Sigma}_b^\mu\}$, and the probabilistic smoothed statistics, $\{\tilde{\boldsymbol{\mu}}_b^\mu, \tilde{\boldsymbol{\mu}}_b^\Sigma, \tilde{\boldsymbol{\Sigma}}_b^\mu\}$, cross different epochs. The probabilistic representation $\{\tilde{\mathbf{z}}_i^\mu, \tilde{\mathbf{z}}_i^\Sigma\}$ are then re-parameterized (Kingma & Welling, 2014) into the final representation \mathbf{z}_i , and passed into the final layer (discussed in Sec. 3.4) to generate the prediction and uncertainty estimation. Note that the computation of statistics from multiple \mathbf{x} 's is only needed during training. During testing, VIR directly uses these statistics and therefore does not need to re-compute them.

3.4 CONSTRUCTING $p(y_i|\mathbf{z}_i)$

Our VIR's predictor $p(y_i|\mathbf{z}_i) \triangleq \mathcal{N}(y_i; \hat{y}_i, \hat{s}_i)$ predicts both the mean and variance for y_i by first predicting the NIG distribution and then marginalizing out the latent variables. It is motivated by the following observations on label distribution smoothing (LDS) in (Yang et al., 2021) and deep evidential regression (DER) in (Amini et al., 2020), as well as intuitions on effective counts in conjugate distributions.

LDS's Limitations in Our Probabilistic Imbalanced Regression Setting. The motivation of LDS (Yang et al., 2021) is that the empirical label distribution can not reflect the real label distribution in an imbalanced dataset with a continuous label space; consequently, reweighting methods for imbalanced regression fail due to these inaccurate label densities. By applying a smoothing kernel on the empirical label distribution, LDS tries to recover the effective label distribution, with which reweighting methods can obtain 'better' weights to improve imbalanced regression. However, in our probabilistic imbalanced regression, one needs to consider both (1) prediction accuracy for the data with minority labels and (2) uncertainty estimation for each model. Unfortunately, LDS only focuses on improving the accuracy, especially for the data with minority labels, and therefore does not provide uncertainty estimation, which is crucial to assess the predictions' reliability.

DER's Limitations in Our Probabilistic Imbalanced Regression Setting. In DER (Amini et al., 2020), the predicted labels with their correspond uncertainties are represented by the approximate

posterior parameters $(\gamma, \nu, \alpha, \beta)$ of the Normal Inverse Gamma (NIG) distribution $NIG(\gamma, \nu, \alpha, \beta)$. A DER model is trained via minimizing the negative log-likelihood (NLL) of a Student-t distribution:

$$\mathcal{L}_i^{DER} = \frac{1}{2} \log\left(\frac{\pi}{\nu}\right) + \left(\alpha + \frac{1}{2}\right) \log((y_i - \gamma)^2 \nu + \Omega) - \alpha \log(\Omega) + \log\left(\frac{\Gamma(\alpha)}{\Gamma(\alpha + \frac{1}{2})}\right), \quad (3)$$

where $\Omega = 2\beta(1 + \nu)$. It is therefore nontrivial to properly incorporate a reweighting mechanism into the NLL. One straightforward approach is to directly reweight \mathcal{L}_i^{DER} for different data points (\mathbf{x}_i, y_i) . However, this contradicts the formulation of NIG and often leads to poor performance, as we verify in Sec. 5.

Intuition of Pseudo-Counts for VIR. To properly incorporate different reweighting methods, our VIR relies on the intuition of pseudo-counts (pseudo-observations) in conjugate distributions (Bishop, 2006). Assuming Gaussian likelihood, the *conjugate distributions* would be an NIG distribution (Bishop, 2006), i.e., $(\mu, \Sigma) \sim NIG(\gamma, \nu, \alpha, \beta)$, which means:

$$\mu \sim \mathcal{N}(\gamma, \Sigma/\nu), \quad \Sigma \sim \Gamma^{-1}(\alpha, \beta),$$

where $\Gamma^{-1}(\alpha, \beta)$ is an inverse gamma distribution. With an NIG prior distribution $NIG(\gamma_0, \nu_0, \alpha_0, \beta_0)$, the posterior distribution of the NIG after observing n real data points $\{u_i\}_{i=1}^n$ are:

$$\gamma_n = \frac{\gamma_0 \nu_0 + n \bar{u}}{\nu_n}, \quad \nu_n = \nu_0 + n, \quad \alpha_n = \alpha_0 + \frac{n}{2}, \quad \beta_n = \beta_0 + \frac{1}{2}(\gamma_0^2 \nu_0) + \Phi, \quad (4)$$

where $\bar{u} = \frac{1}{n} \sum_i u_i$ and $\Phi = \frac{1}{2}(\sum_i u_i^2 - \gamma_n^2 \nu_n)$. Here ν_0 and α_0 can be interpreted as virtual observations, i.e., *pseudo-counts or pseudo-observations* that contribute to the posterior distribution. Overall, the mean of posterior distribution above can be interpreted as an estimation from $(2\alpha_0 + n)$ observations, with $2\alpha_0$ virtual observations and n real observations. Similarly, the variance can be interpreted as an estimation from $(\nu + n)$ observations. This intuition is crucial in developing the predictor of our VIR.

From Pseudo-Counts to Balanced Predictive Distributions. Based on the intuition above, we construct our predictor (i.e., $p(y_i|\mathbf{z}_i)$) by (1) generating the parameters in the posterior distribution of NIG, (2) computing re-weighted parameters by imposing the importance weights obtained from LDS, and (3) producing the final prediction with corresponding uncertainty estimation.

Based on Eqn. 4, we feed the final representation $\{\mathbf{z}_i\}_{i=1}^N$ generated from the Sec. 3.3 (Eqn. 2) into a linear layer to output the intermediate parameters n_i, Ψ_i, Φ_i for data point (\mathbf{x}_i, y_i) :

$$n_i, \Psi_i, \Phi_i = \mathcal{G}(\mathbf{z}_i), \quad \mathbf{z}_i \sim q(\mathbf{z}_i|\{\mathbf{x}_i\}_{i=1}^N) = \mathcal{N}(\mathbf{z}_i; \tilde{\mathbf{z}}_i^\mu, \tilde{\mathbf{z}}_i^\Sigma)$$

We then apply the importance weights $\sum_{b' \in \mathcal{B}} k(y_b, y_{b'})^{-\frac{1}{2}}$ calculated from the smoothed label distribution to the *pseudo-count* n_i to produce the re-weighted parameters of posterior distribution of NIG. Along with the pre-defined prior parameters $(\gamma_0, \nu_0, \alpha_0, \beta_0)$, we are able to compute the parameters of posterior distribution $NIG(\gamma_i, \nu_i, \alpha_i, \beta_i)$ for (\mathbf{x}_i, y_i) :

$$\begin{aligned} \gamma_i^* &= \frac{\gamma_0 \nu_0 + \left(\sum_{b' \in \mathcal{B}} k(y_b, y_{b'})\right)^{-\frac{1}{2}} \cdot n_i \Psi_i}{\nu_i^*}, & \nu_i^* &= \nu_0 + \left(\sum_{b' \in \mathcal{B}} k(y_b, y_{b'})\right)^{-\frac{1}{2}} \cdot n_i, \\ \alpha_i^* &= \alpha_0 + \left(\sum_{b' \in \mathcal{B}} k(y_b, y_{b'})\right)^{-\frac{1}{2}} \cdot \frac{n_i}{2}, & \beta_i^* &= \beta_0 + \frac{1}{2}(\gamma_0^2 \nu_0) + \Phi_i. \end{aligned}$$

Based on the NIG posterior distribution, we can then compute final prediction and uncertainty estimation as

$$\hat{y}_i = \gamma_i^*, \quad \hat{s}_i = \frac{\beta_i^*}{\nu_i^* (\alpha_i^* - 1)}.$$

We use an objective function similar to Eqn. 3, but with different definitions of $(\gamma, \nu, \alpha, \beta)$, to optimize our VIR model:

$$\mathcal{L}_i^P = \mathbb{E}_{q_\phi(\mathbf{z}_i|\{\mathbf{x}_i\}_{i=1}^N)} \left[\frac{1}{2} \log\left(\frac{\pi}{\nu_i^*}\right) + \left(\alpha_i^* + \frac{1}{2}\right) \log((y_i - \gamma_i^*)^2 \nu_i^* + \Omega) - \alpha_i^* \log(\omega_i^*) + \log\left(\frac{\Gamma(\alpha_i^*)}{\Gamma(\alpha_i^* + \frac{1}{2})}\right) \right], \quad (5)$$

where $\omega_i^* = 2\beta_i^*(1 + \nu_i^*)$. Note that \mathcal{L}_i^P is part of the ELBO in Eqn. 1. Similar to (Amini et al., 2020), we use an additional regularization term to achieve better accuracy¹:

$$\mathcal{L}_i^R = (\nu + 2\alpha) \cdot |y_i - \hat{y}_i|.$$

\mathcal{L}_i^P and \mathcal{L}_i^R together constitute the objective function for learning the predictor $p(\mathbf{y}_i|\mathbf{z}_i)$.

¹Note that in DER, the total evidence Φ has a value $2\nu + \alpha$, but to the best of our knowledge, it would be more reasonable to use $\nu + 2\alpha$ as the total evidence for an NIG distribution (Bishop, 2006).

Table 1: Accuracy on AgeDB-DIR.

Metrics	MAE ↓				GM ↓			
	all	many	medium	few	all	many	medium	few
VANILLA (Yang et al., 2021)	7.77	6.62	9.55	13.67	5.05	4.23	7.01	10.75
VAE (Kingma & Welling, 2014)	7.63	6.58	9.21	13.45	4.86	4.11	6.61	10.24
DEEP ENS. (Lakshminarayanan et al., 2017)	7.73	6.62	9.37	13.90	4.87	4.37	6.50	11.35
INFER NOISE (Mi et al., 2022a)	8.53	7.62	9.73	13.82	5.57	4.95	6.58	10.86
SMOTER (Torgo et al., 2013)	8.16	7.39	8.65	12.28	5.21	4.65	5.69	8.49
SMOEN (Branco et al., 2017)	8.26	7.64	9.01	12.09	5.36	4.9	6.19	8.44
SQINV (Yang et al., 2021)	7.81	7.16	8.80	11.2	4.99	4.57	5.73	7.77
DER (Amini et al., 2020)	8.09	7.31	8.99	12.66	5.19	4.59	6.43	10.49
LDS (Yang et al., 2021)	7.67	6.98	8.86	10.89	4.85	4.39	5.8	7.45
FDS (Yang et al., 2021)	7.69	7.10	8.86	9.98	4.83	4.41	5.97	6.29
LDS + FDS (Yang et al., 2021)	7.55	7.01	8.24	10.79	4.72	4.36	5.45	6.79
RANKSIM (Gong et al., 2022)	7.02	6.49	7.84	9.68	4.53	4.13	5.37	6.89
LDS + FDS + DER (Amini et al., 2020)	8.18	7.44	9.52	11.45	5.30	4.75	6.74	7.68
VIR (OURS)	6.99	6.39	7.47	9.51	4.41	4.07	5.05	6.23
OURS vs. VANILLA	+0.78	+0.23	+2.08	+4.16	+0.64	+0.16	+1.96	+4.52
OURS vs. INFER NOISE	+1.54	+1.23	+2.26	+4.31	+1.16	+0.88	+1.53	+4.63
OURS vs. DER	+1.10	+0.92	+1.52	+3.15	+0.78	+0.52	+1.38	+4.26
OURS vs. LDS + FDS	+0.56	+0.62	+0.77	+1.28	+0.31	+0.29	+0.40	+0.56
OURS vs. RANKSIM	+0.03	+0.10	+0.37	+0.17	+0.12	+0.06	+0.32	+0.66

Table 2: Accuracy on IW-DIR.

Metrics	MAE ↓				GM ↓			
	All	Many	Medium	Few	All	Many	Medium	Few
VANILLA (Yang et al., 2021)	8.06	7.23	15.12	26.33	4.57	4.17	10.59	20.46
VAE (Kingma & Welling, 2014)	8.04	7.20	15.05	26.30	4.57	4.22	10.56	20.72
DEEP ENS. (Lakshminarayanan et al., 2017)	8.08	7.31	15.09	26.47	4.59	4.26	10.61	21.13
INFER NOISE (Mi et al., 2022a)	8.11	7.36	15.23	26.29	4.68	4.33	10.65	20.31
SMOTER (Torgo et al., 2013)	8.14	7.42	14.15	25.28	4.64	4.30	9.05	19.46
SMOEN (Branco et al., 2017)	8.03	7.30	14.02	25.93	4.63	4.30	8.74	20.12
SQINV (Yang et al., 2021)	7.87	7.24	12.44	22.76	4.47	4.22	7.25	15.10
DER (Amini et al., 2020)	7.85	7.18	13.35	24.12	4.47	4.18	8.18	15.18
LDS (Yang et al., 2021)	7.83	7.31	12.43	22.51	4.42	4.19	7.00	13.94
FDS (Yang et al., 2021)	7.83	7.23	12.60	22.37	4.42	4.20	6.93	13.48
LDS + FDS (Yang et al., 2021)	7.78	7.20	12.61	22.19	4.37	4.12	7.39	12.61
RANKSIM (Gong et al., 2022)	7.50	6.93	12.09	21.68	4.19	3.97	6.65	13.28
LDS + FDS + DER (Amini et al., 2020)	7.24	6.64	11.87	23.44	3.93	3.69	6.64	16.00
VIR (OURS)	7.19	6.56	11.81	20.96	3.85	3.63	6.51	12.23
OURS vs. VANILLA	+0.87	+0.67	+3.31	+5.37	+0.72	+0.54	+4.08	+8.23
OURS vs. INFER NOISE	+0.92	+0.80	+3.42	+5.33	+0.83	+0.70	+4.14	+8.08
OURS vs. DER	+0.66	+0.62	+1.54	+3.16	+0.62	+0.55	+1.67	+2.95
OURS vs. LDS + FDS	+0.59	+0.64	+0.8	+1.23	+0.52	+0.49	+0.88	+0.38
OURS vs. RANKSIM	+0.31	+0.37	+0.28	+0.72	+0.34	+0.34	+0.14	+1.05

3.5 FINAL OBJECTIVE FUNCTION

Putting together Sec. 3.3 and Sec. 3.4, our final objective function (to minimize) for VIR is:

$$\mathcal{L}^{VIR} = \sum_{i=1}^N \mathcal{L}_i^{VIR}, \quad \mathcal{L}_i^{VIR} = \lambda \mathcal{L}_i^{\mathcal{R}} - \mathcal{L}(\theta, \phi; \mathbf{x}_i, y_i) = \lambda \mathcal{L}_i^{\mathcal{R}} - \mathcal{L}_i^{\mathcal{P}} - \mathcal{L}_i^{\mathcal{D}} + \mathcal{L}_i^{\mathcal{KL}},$$

where $\mathcal{L}(\theta, \phi; \mathbf{x}_i, y_i) = \mathcal{L}_i^{\mathcal{P}} + \mathcal{L}_i^{\mathcal{D}} - \mathcal{L}_i^{\mathcal{KL}}$ is the ELBO in Eqn. 1. λ adjusts the importance of the additional regularizer and the ELBO, and thus lead to a better result both on accuracy and uncertainty estimation.

4 DISCUSSIONS

In this section, we discuss intuition of our methods (see more discussion in the Supplementary).

4.1 DISCUSSION ON I.I.D. AND N.I.D. ASSUMPTIONS

Generalization Error, Bias, and Variance. We could analyze the generalization error of our VIR by bounding the generalization with the sum of three terms: (a) the bias of our estimator, (2) the variance of our estimator, (3) model complexity. Essentially VIR uses the N.I.D. assumption increases our estimator’s bias, but significantly reduces its variance in the imbalanced setting. Since the model complexity is kept the same (using the same backbone neural network) as the baselines, N.I.D. will lead to a lower generalization error.

Variance of Estimators in Imbalanced Settings. In the imbalanced setting, one typically use inverse weighting to produced an unbiased estimator (i.e., making the first term of the aforementioned bound zero). However, for data with extremely low density, its inverse would be extremely large, therefore leading to a very large variance for the estimator. Our VIR replaces I.I.D. with N.I.D. to “smooth out” such singularity, and therefore significantly lowers the variance of the estimator (i.e., making the second term of the aforementioned bound smaller), and ultimately lowers the generalization error.

4.2 INTUITION ON WHY VIR PERFORMS BETTER THAN DIR

Our VIR outperforms DIR because:

- DIR uses deterministic representations, with one vector as the final representation for each data point. In contrast, our VIR uses probabilistic representations, with one vector as the mean of the representation and another vector as the variance of the representation. Such dual representation is more robust to noise and therefore leads to better prediction performance.
- DIR is a deterministic model, while our VIR is a Bayesian model. Essentially VIR is equivalent to sampling infinitely many predictions for each input data point and averaging these predictions. Therefore intuitively it makes sense that VIR could lead to better prediction performance.

- It is also worth noting that DIR is a deterministic model and therefore cannot produce uncertainty estimation. In contrast, Our VIR formulates a probabilistic deep generative model for imbalanced data, and therefore can naturally produce both more accurate predictions compared to DIR (Yang et al., 2021) and better uncertainty estimation compared to DER (Amini et al., 2020).

5 EXPERIMENTS

Datasets. We evaluate our methods in terms of prediction accuracy and uncertainty estimation on four imbalanced datasets², AgeDB-DIR (Moschoglou et al., 2017), IMDB-WIKI-DIR (Rothe et al., 2018), STS-B-DIR (Cer et al., 2017), and NYUD2-DIR (Silberman et al., 2012). Due to page limit, results for NYUD2-DIR (Silberman et al., 2012) are moved to the Supplementary. We follow the preprocessing procedures in DIR (Yang et al., 2021). Details for each datasets are in the Supplementary, and please refer to (Yang et al., 2021) for details on label density distributions and levels of imbalance.

Baselines. We use ResNet-50 (He et al., 2016) (for AgeDB-DIR and IMDB-WIKI-DIR) and BiLSTM (Huang et al., 2015) (for STS-B-DIR) as our backbone networks, and more details for baseline are in the supplement. we describe the baselines below.

- *Vanilla*: We use the term **VANILLA** to denote a plain model without adding any approaches.
- *Synthetic-Sample-Based Methods*: Various existing imbalanced regression methods are also included as baselines; these include Deep Ensemble (Lakshminarayanan et al., 2017), Infer Noise (Mi et al., 2022a), SMOTER (Torgo et al., 2013), and SMOGN (Branco et al., 2017).
- *Cost-Sensitive Reweighting*: As shown in DIR (Yang et al., 2021), the square-root weighting variant (SQINV) baseline (i.e., $(\sum_{b' \in \mathcal{B}} k(y_b, y_{b'}))^{-\frac{1}{2}}$) always outperforms Vanilla. Therefore, for fair comparison, *all* our experiments (for both baselines and VIR) use SQINV weighting.

Evaluation Metrics. We follow the evaluation metrics in (Yang et al., 2021) to evaluate the accuracy of our proposed methods; these include Mean Absolute Error (MAE), Mean Squared Error (MSE). Furthermore, for AgeDB-DIR and IMDB-WIKI-DIR, we use Geometric Mean (GM) to evaluate the accuracy; for STS-B-DIR, we use Pearson correlation and Spearman correlation. We use typical evaluation metrics for uncertainty estimation in regression problems to evaluate our produced uncertainty estimation; these include Negative Log Likelihood (NLL), Area Under Sparsification Error (AUSE). Eqn. 5 shows the formula for NLL, and more details regarding to AUSE can be found in (Ilg et al., 2018). We also include calibrated uncertainty results for VIR in the Supplementary.

Evaluation Process. Following (Liu et al., 2019; Yang et al., 2021), for a data sample x_i with its label y_i which falls into the target bins b_i , we divide the label space into three disjoint subsets: many-shot region $\{b_i \in \mathcal{B} \mid y_i \in b_i \ \& \ |y_i| > 100\}$, medium-shot region $\{b_i \in \mathcal{B} \mid y_i \in b_i \ \& \ 20 \leq |y_i| \leq 100\}$, and few-shot region $\{b_i \in \mathcal{B} \mid y_i \in b_i \ \& \ |y_i| < 20\}$, where $|\cdot|$ denotes the cardinality of the set. We report results on the overall test set and these subsets with the accuracy metrics and uncertainty metrics discussed above.

Implementation Details. We conducted five separate trials for our method using different random seeds. The error bars and other implementation details are included in the Supplementary.

Table 3: Accuracy on STS-B-DIR.

Metrics	MSE ↓				Pearson ↑			
	All	Many	Medium	Few	All	Many	Medium	Few
VANILLA (Yang et al., 2021)	0.974	0.851	1.520	0.984	0.742	0.720	0.627	0.752
VAE (Kingma & Welling, 2014)	0.968	0.833	1.511	1.102	0.751	0.724	0.621	0.749
DEEP ENS. (Lakshminarayanan et al., 2017)	0.972	0.846	1.496	1.032	0.746	0.723	0.619	0.750
INFER NOISE (Mi et al., 2022a)	0.954	0.980	1.408	0.967	0.747	0.711	0.631	0.756
SMOTER (Torgo et al., 2013)	1.046	0.924	1.542	1.154	0.726	0.693	0.653	0.706
SMOGN (Branco et al., 2017)	0.990	0.896	1.327	1.175	0.732	0.704	0.655	0.692
INV (Yang et al., 2021)	1.005	0.894	1.482	1.046	0.728	0.703	0.625	0.732
DER (Amini et al., 2020)	1.001	0.912	1.368	1.055	0.732	0.711	0.646	0.742
LDS (Yang et al., 2021)	0.914	0.819	1.319	0.955	0.756	0.734	0.638	0.762
FDS (Yang et al., 2021)	0.927	0.851	1.225	1.012	0.750	0.724	0.667	0.742
LDS + FDS (Yang et al., 2021)	0.907	0.802	1.363	0.942	0.760	0.740	0.652	0.766
RANKSIM (Gong et al., 2022)	0.903	0.908	0.911	0.804	0.758	0.706	0.690	0.827
LDS + FDS + DER (Amini et al., 2020)	1.007	0.880	1.535	1.086	0.729	0.714	0.635	0.731
VIR (OURS)	0.892	0.795	0.899	0.781	0.776	0.752	0.696	0.845
OURS VS. VANILLA	+0.082	+0.056	+0.621	+0.203	+0.034	+0.032	+0.069	+0.093
OURS VS. INFER NOISE	+0.062	+0.185	+0.509	+0.186	+0.029	+0.041	+0.065	+0.089
OURS VS. DER	+0.109	+0.117	+0.469	+0.274	+0.044	+0.041	+0.050	+0.103
OURS VS. LDS + FDS	+0.015	+0.007	+0.464	+0.161	+0.016	+0.012	+0.044	+0.079
OURS VS. RANKSIM	+0.011	+0.113	+0.012	+0.023	+0.018	+0.046	+0.006	+0.018

²Among the five datasets proposed in (Yang et al., 2021), only four of them are publicly available.

Table 4: Uncertainty estimation on AgeDB-DIR.

Metrics	NLL ↓				AUSE ↓			
	All	Many	Med	Few	All	Many	Med	Few
DEEP ENS. (Lakshminarayanan et al., 2017)	5.311	4.031	6.726	8.523	0.541	0.626	0.466	0.483
INFER NOISE (Mi et al., 2022a)	4.616	4.413	4.866	5.842	0.465	0.458	0.457	0.496
DER (Amini et al., 2020)	3.918	3.741	3.919	4.432	0.523	0.464	0.449	0.486
LDS + FDS + DER (Amini et al., 2020)	3.787	3.689	3.912	4.234	0.451	0.460	0.399	0.565
VIR (OURS)	3.703	3.598	3.805	4.196	0.434	0.456	0.324	0.414
Ours vs. DER	+0.215	+0.143	+0.114	+0.236	+0.089	+0.008	+0.125	+0.072
Ours vs. LDS + FDS + DER	+0.084	+0.091	+0.107	+0.038	+0.017	+0.004	+0.075	+0.151

Table 5: Uncertainty estimation on IW-DIR.

Metrics	NLL ↓				AUSE ↓			
	All	Many	Medium	Few	All	Many	Medium	Few
DEEP ENS. (Lakshminarayanan et al., 2017)	5.219	4.102	7.123	8.852	0.846	0.862	0.745	0.718
INFER NOISE (Mi et al., 2022a)	4.231	4.078	5.326	8.292	0.732	0.728	0.561	0.478
DER (Amini et al., 2020)	3.850	3.699	4.997	6.638	0.813	0.802	0.650	0.541
LDS + FDS + DER (Amini et al., 2020)	3.683	3.602	4.391	5.697	0.784	0.670	0.459	0.483
VIR (OURS)	3.651	3.579	4.296	5.518	0.634	0.649	0.434	0.379
Ours vs. DER	+0.199	+0.120	+0.701	+1.120	+0.179	+0.153	+0.216	+0.162
Ours vs. LDS + FDS + DER	+0.032	+0.023	+0.095	+0.179	+0.150	+0.021	+0.025	+0.104

5.1 IMBALANCED REGRESSION ACCURACY

We report the accuracy of different methods in Table 1, Table 2, and Table 3 for AgeDB-DIR, IMDB-WIKI-DIR and STS-B-DIR, respectively. In all the tables, we can observe that our VIR consistently outperforms all baselines in all metrics.

As shown in the last four rows of all three tables, our proposed VIR compares favorably against strong baselines including DIR variants (Yang et al., 2021) and DER (Amini et al., 2020), Infer Noise (Mi et al., 2022a), and RankSim (Gong et al., 2022), especially on the imbalanced data samples (i.e., in the few-shot columns). Notably, VIR improves upon the state-of-the-art method RankSim by 9.6% and 7.9% on AgeDB-DIR and IMDB-WIKI-DIR, respectively, in terms of few-shot GM. This verifies the effectiveness of our methods in terms of overall performance. More accuracy results on different metrics are included in the Supplementary. Besides the main results, we also include ablation studies for VIR in the Supplementary, showing the effectiveness of VIR’s encoder and predictor.

5.2 IMBALANCED REGRESSION UNCERTAINTY ESTIMATION

Different from DIR (Yang et al., 2021) which only focuses on accuracy, we create a new benchmark for uncertainty estimation in imbalanced regression. Table 4, Table 5, and Table 6 show the results on uncertainty estimation for three datasets AgeDB-DIR, IMDB-WIKI-DIR, and STS-B-DIR, respectively. Note that most baselines from Table 1, Table 2, and Table 3 are *deterministic* methods (as opposed to probabilistic methods like ours) and *cannot provide uncertainty estimation*; therefore they are not applicable here. To show the superiority of our VIR model, we create a strongest baseline by concatenating the DIR variants (LDS + FDS) with the DER (Amini et al., 2020).

Results show that our VIR consistently outperforms all baselines across different metrics, especially in the few-shot metrics. Note that our proposed methods mainly focus on the imbalanced setting, and therefore naturally places more emphasis on the few-shot metrics. Notably, on AgeDB-DIR, IMDB-WIKI-DIR, and STS-B-DIR, our VIR improves upon the strongest baselines, by 14.2% ~ 17.1% in terms of few-shot AUSE.

5.3 LIMITATIONS

Although our methods successfully improve both accuracy and uncertainty estimation on imbalanced regression, there are still several limitations. Exactly computing *variance of the variances* in Sec. 3.3 is challenging; we therefore resort to fixed variance as an approximation. Developing more accurate and efficient approximations would also be interesting future work.

6 CONCLUSION

We identify the problem of probabilistic deep imbalanced regression, which aims to both improve accuracy and obtain reasonable uncertainty estimation in imbalanced regression. We propose VIR, which can use any deep regression models as backbone networks. VIR borrows data with similar regression labels to produce the probabilistic representations and modulates the conjugate distributions to impose probabilistic reweighting on imbalanced data. Furthermore, we create new benchmarks for uncertainty estimation on imbalanced regression. Experiments show that our methods outperform

Table 6: Uncertainty estimation on STS-B-DIR.

Metrics	NLL ↓				AUSE ↓			
	All	Many	Medium	Few	All	Many	Medium	Few
DEEP ENS. (Lakshminarayanan et al., 2017)	3.913	3.911	4.223	4.106	0.709	0.621	0.676	0.663
INFER NOISE (Mi et al., 2022a)	3.748	3.753	3.755	3.688	0.673	0.631	0.644	0.639
DER (Amini et al., 2020)	2.667	2.601	3.013	2.401	0.682	0.583	0.613	0.624
LDS + FDS + DER (Amini et al., 2020)	2.561	2.514	2.880	2.358	0.672	0.581	0.609	0.615
VIR (OURS)	1.996	1.810	2.754	2.152	0.591	0.575	0.602	0.510
Ours vs. DER	+0.671	+0.791	+0.259	+0.249	+0.091	+0.008	+0.011	+0.114
Ours vs. LDS + FDS + DER	+0.565	+0.704	+0.126	+0.206	+0.081	+0.006	+0.007	+0.105

state-of-the-art imbalanced regression models in terms of both accuracy and uncertainty estimation. Future work may include (1) improving VIR by better approximating *variance of the variances* in probability distributions, and (2) developing novel approaches that can achieve stable performance even on imbalanced data with limited sample size, and (3) exploring techniques such as mixture density networks (Bishop, 1994) to enable multi-modality in the latent distribution, thereby further improving the performance.

REFERENCES

- Alexander Amini, Wilko Schwarting, Ava Soleimany, and Daniela Rus. Deep evidential regression. *Advances in Neural Information Processing Systems*, 33:14927–14937, 2020.
- Christopher M Bishop. Mixture density networks. 1994.
- Christopher M Bishop. *Pattern recognition and machine learning*. springer, 2006.
- Paula Branco, Luís Torgo, and Rita P Ribeiro. Smogn: a pre-processing approach for imbalanced regression. In *First international workshop on learning with imbalanced domains: Theory and applications*, pp. 36–50. PMLR, 2017.
- Paula Branco, Luis Torgo, and Rita P Ribeiro. Rebagg: Resampled bagging for imbalanced regression. In *Second International Workshop on Learning with Imbalanced Domains: Theory and Applications*, pp. 67–81. PMLR, 2018.
- Daniel Cer, Mona Diab, Eneko Agirre, Iñigo Lopez-Gazpio, and Lucia Specia. Semeval-2017 task 1: Semantic textual similarity multilingual and crosslingual focused evaluation. In *Proceedings of the 11th International Workshop on Semantic Evaluation*, pp. 1–14, 2017.
- Bertrand Charpentier, Oliver Borchert, Daniel Zügner, Simon Geisler, and Stephan Günnemann. Natural posterior network: Deep bayesian predictive uncertainty for exponential family distributions. In *The Tenth International Conference on Learning Representations, ICLR 2022, Virtual Event, April 25-29, 2022*. OpenReview.net, 2022.
- Nitesh V Chawla, Kevin W Bowyer, Lawrence O Hall, and W Philip Kegelmeyer. Smote: synthetic minority over-sampling technique. *Journal of artificial intelligence research*, 16:321–357, 2002.
- Zongyong Deng, Hao Liu, Yaoxing Wang, Chenyang Wang, Zekuan Yu, and Xuehong Sun. PML: progressive margin loss for long-tailed age classification. In *IEEE Conference on Computer Vision and Pattern Recognition, CVPR 2021, virtual, June 19-25, 2021, 2021*.
- Yarin Gal and Zoubin Ghahramani. Dropout as a bayesian approximation: Representing model uncertainty in deep learning. In *Proceedings of the 33rd International Conference on Machine Learning, ICML 2016, New York City, NY, USA, June 19-24, 2016*, volume 48 of *JMLR Workshop and Conference Proceedings*, pp. 1050–1059. JMLR.org, 2016.
- Yu Gong, Greg Mori, and Frederick Tung. Ranksim: Ranking similarity regularization for deep imbalanced regression. In *International Conference on Machine Learning, ICML 2022, 17-23 July 2022, Baltimore, Maryland, USA*, volume 162 of *Proceedings of Machine Learning Research*, pp. 7634–7649. PMLR, 2022.
- Arjun K Gupta and Daya K Nagar. *Matrix variate distributions*, volume 104. CRC Press, 2018.
- Kaiming He, Xiangyu Zhang, Shaoqing Ren, and Jian Sun. Deep residual learning for image recognition. In *2016 IEEE Conference on Computer Vision and Pattern Recognition, CVPR 2016, Las Vegas, NV, USA, June 27-30, 2016*, pp. 770–778. IEEE Computer Society, 2016.
- Jakob Heiss, Jakob Weissteiner, Hanna Wutte, Sven Seuken, and Josef Teichmann. Nomu: Neural optimization-based model uncertainty. *arXiv preprint arXiv:2102.13640*, 2021.
- Zhiheng Huang, Wei Xu, and Kai Yu. Bidirectional LSTM-CRF models for sequence tagging. *CoRR*, 2015.
- Eyke Hüllermeier and Willem Waegeman. Aleatoric and epistemic uncertainty in machine learning: A tutorial introduction. *CoRR*, abs/1910.09457, 2019.

-
- Eddy Ilg, Özgün cCiccek, Silvio Galesso, Aaron Klein, Osama Makansi, Frank Hutter, and Thomas Brox. Uncertainty estimates and multi-hypotheses networks for optical flow. In *Computer Vision - ECCV 2018 - 15th European Conference, Munich, Germany, September 8-14, 2018, Proceedings, Part VII*, volume 11211 of *Lecture Notes in Computer Science*, pp. 677–693. Springer, 2018.
- Haoming Jiang, Pengcheng He, Weizhu Chen, Xiaodong Liu, Jianfeng Gao, and Tuo Zhao. SMART: robust and efficient fine-tuning for pre-trained natural language models through principled regularized optimization. In Dan Jurafsky, Joyce Chai, Natalie Schluter, and Joel R. Tetreault (eds.), *Proceedings of the 58th Annual Meeting of the Association for Computational Linguistics, ACL 2020, Online, July 5-10, 2020*, pp. 2177–2190. Association for Computational Linguistics, 2020.
- Alex Kendall and Yarin Gal. What uncertainties do we need in bayesian deep learning for computer vision? *arXiv preprint arXiv:1703.04977*, 2017.
- Diederik P. Kingma and Max Welling. Auto-encoding variational bayes. In *2nd International Conference on Learning Representations, ICLR 2014, Banff, AB, Canada, April 14-16, 2014, Conference Track Proceedings*, 2014.
- Volodymyr Kuleshov, Nathan Fenner, and Stefano Ermon. Accurate uncertainties for deep learning using calibrated regression. In *International Conference on Machine Learning*, pp. 2796–2804. PMLR, 2018.
- Balaji Lakshminarayanan, Alexander Pritzel, and Charles Blundell. Simple and scalable predictive uncertainty estimation using deep ensembles. In *Advances in Neural Information Processing Systems 30: Annual Conference on Neural Information Processing Systems 2017, December 4-9, 2017, Long Beach, CA, USA*, pp. 6402–6413, 2017.
- Jeremiah Liu, Zi Lin, Shreyas Padhy, Dustin Tran, Tania Bedrax Weiss, and Balaji Lakshminarayanan. Simple and principled uncertainty estimation with deterministic deep learning via distance awareness. In *Advances in Neural Information Processing Systems*, volume 33. Curran Associates, Inc., 2020.
- Ziwei Liu, Zhongqi Miao, Xiaohang Zhan, Jiayun Wang, Boqing Gong, and Stella X. Yu. Large-scale long-tailed recognition in an open world. In *IEEE Conference on Computer Vision and Pattern Recognition, CVPR 2019, Long Beach, CA, USA, June 16-20, 2019*, pp. 2537–2546. Computer Vision Foundation / IEEE, 2019.
- Lu Mi, Hao Wang, Yonglong Tian, Hao He, and Nir Shavit. Training-free uncertainty estimation for dense regression: Sensitivity as a surrogate. In *AAAI 2022*, pp. 10042–10050. AAAI Press, 2022a.
- Lu Mi, Hao Wang, Yonglong Tian, and Nir Shavit. Training-free uncertainty estimation for neural networks. In *AAAI*, 2022b.
- Stylianios Moschoglou, Athanasios Papaioannou, Christos Sagonas, Jiankang Deng, Irene Kotsia, and Stefanos Zafeiriou. Agedb: The first manually collected, in-the-wild age database. In *2017 IEEE Conference on Computer Vision and Pattern Recognition Workshops, CVPR Workshops 2017, Honolulu, HI, USA, July 21-26, 2017*, pp. 1997–2005, 2017.
- Jiawei Ren, Mingyuan Zhang, Cunjun Yu, and Ziwei Liu. Balanced mse for imbalanced visual regression. In *IEEE/CVF Conference on Computer Vision and Pattern Recognition, CVPR 2022, New Orleans, LA, USA, June 18-24, 2022*, pp. 7916–7925. IEEE, 2022.
- Rasmus Rothe, Radu Timofte, and Luc Van Gool. Deep expectation of real and apparent age from a single image without facial landmarks. *Int. J. Comput. Vis.*, 126(2-4):144–157, 2018.
- Nathan Silberman, Derek Hoiem, Pushmeet Kohli, and Rob Fergus. Indoor segmentation and support inference from rgb-d images. *ECCV (5)*, 7576:746–760, 2012.
- Jasper Snoek, Yaniv Ovadia, Emily Fertig, Balaji Lakshminarayanan, Sebastian Nowozin, D. Sculley, Joshua V. Dillon, Jie Ren, and Zachary Nado. Can you trust your model’s uncertainty? evaluating predictive uncertainty under dataset shift. In *Advances in Neural Information Processing Systems 32: Annual Conference on Neural Information Processing Systems 2019, NeurIPS 2019, December 8-14, 2019, Vancouver, BC, Canada*, pp. 13969–13980, 2019.

-
- Hao Song, Tom Diethe, Meelis Kull, and Peter Flach. Distribution calibration for regression. In *International Conference on Machine Learning*, pp. 5897–5906. PMLR, 2019.
- Maximilian Stadler, Bertrand Charpentier, Simon Geisler, Daniel Zügner, and Stephan Günnemann. Graph posterior network: Bayesian predictive uncertainty for node classification. In *Advances in Neural Information Processing Systems 34: Annual Conference on Neural Information Processing Systems 2021, NeurIPS 2021, December 6-14, 2021, virtual*, pp. 18033–18048, 2021.
- Baochen Sun, Jiashi Feng, and Kate Saenko. Return of frustratingly easy domain adaptation. In *Proceedings of the Thirtieth AAAI Conference on Artificial Intelligence, February 12-17, 2016, Phoenix, Arizona, USA*, pp. 2058–2065. AAAI Press, 2016.
- Luís Torgo, Rita P. Ribeiro, Bernhard Pfahringer, and Paula Branco. SMOTE for regression. In Luís Correia, Luís Paulo Reis, and José Cascalho (eds.), *Progress in Artificial Intelligence - 16th Portuguese Conference on Artificial Intelligence, EPIA 2013, Angra do Heroísmo, Azores, Portugal, September 9-12, 2013. Proceedings*, volume 8154 of *Lecture Notes in Computer Science*, pp. 378–389. Springer, 2013.
- Joost van Amersfoort, Lewis Smith, Andrew Jesson, Oscar Key, and Yarin Gal. Improving deterministic uncertainty estimation in deep learning for classification and regression. *CoRR*, abs/2102.11409, 2021.
- Yuzhe Yang, Kaiwen Zha, Ying-Cong Chen, Hao Wang, and Dina Katabi. Delving into deep imbalanced regression. In Marina Meila and Tong Zhang (eds.), *Proceedings of the 38th International Conference on Machine Learning, ICML 2021, 18-24 July 2021, Virtual Event*, volume 139 of *Proceedings of Machine Learning Research*, pp. 11842–11851. PMLR, 2021.
- Wei Yin, Jianming Zhang, Oliver Wang, Simon Niklaus, Long Mai, Simon Chen, and Chunhua Shen. Learning to recover 3d scene shape from a single image. In *IEEE Conference on Computer Vision and Pattern Recognition, CVPR 2021, virtual, June 19-25, 2021*, pp. 204–213. Computer Vision Foundation / IEEE, 2021.
- Eric Zelikman, Christopher Healy, Sharon Zhou, and Anand Avati. Crude: calibrating regression uncertainty distributions empirically. *arXiv preprint arXiv:2005.12496*, 2020.
- Zizhao Zhang, Adriana Romero, Matthew J Muckley, Pascal Vincent, Lin Yang, and Michal Drozdal. Reducing uncertainty in undersampled mri reconstruction with active acquisition. In *Proceedings of the IEEE/CVF Conference on Computer Vision and Pattern Recognition*, pp. 2049–2058, 2019.